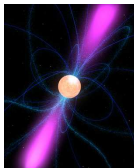


EXPLORING THE
GALACTIC MAGNETIC FIELD
WITH
LOFAR



CHARLOTTE SOBEY
MAX-PLANCK-INSTITUT FÜR RADIOASTRONOMIE
14TH MAY 2013

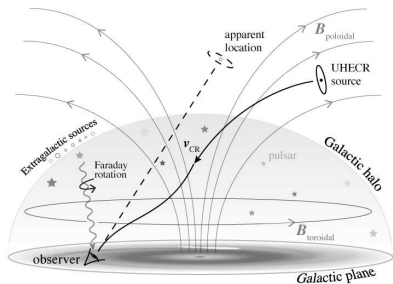
Outline

- μG field of Milky Way ISM
- Faraday rotation
- Ionosphere calibration
- LOFAR RMs
- Aside: element beam



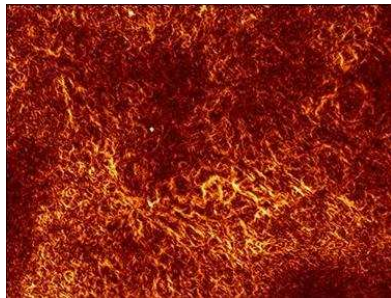
Galactic Magnetic Field

- Why? **Important** for long list of astrophysical processes...



* Actual UHECR trajectory and magnetic-field configuration may vary

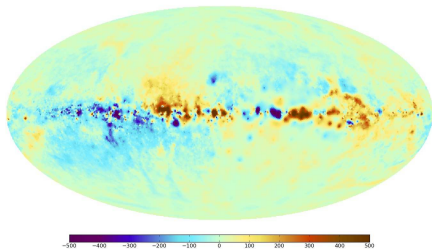
HECR deflection cartoon [A. Noutsos]



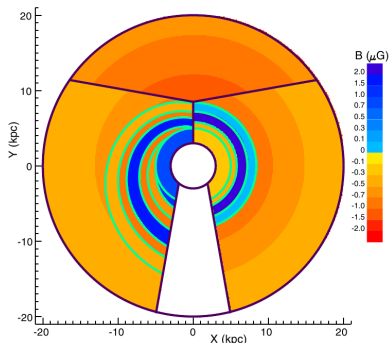
Supersonic ISM turbulence [B. Gaensler]

Measuring the GMF

- How? Faraday Rotation; $\chi = \chi_0 + RM\lambda^2$
- $\langle B_{\parallel} \rangle_{n_e} = 1.232 \mu\text{G} \frac{RM=0.81 \int_{\oplus}^{\oplus} n_e B_{\parallel} dl \text{ (rad m}^{-2}\text{)}}{DM=\int_{\oplus}^{\oplus} n_e dl \text{ (cm}^{-3} \text{ pc)}}$
- **Improvements**; sample size, precision & accuracy



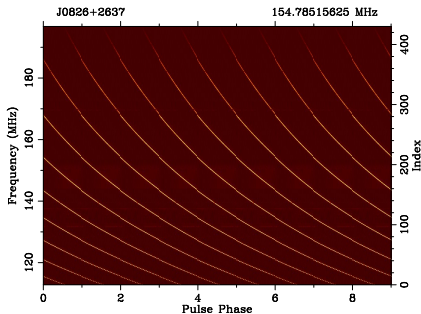
Faraday sky [Oppermann et al. 2011]



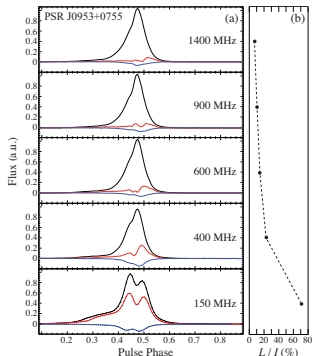
GMF best fit [van Eck et al. 2011]

LOFAR pulsar observations

- Highest quality, low frequency polarisation profiles (c.f. A. Noutsos)
- >20 core stations, large bandwidth (90 MHz), raw data >80 GB/min



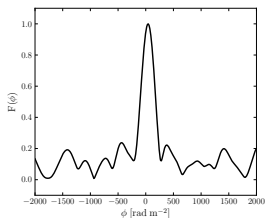
Pulse dispersion [Pilia et al. in prep.]



Evolving pulse profile; Arecibo (1400), Jodrell ([9,6,4]00), LOFAR (150) [A. Noutsos]

RM-synthesis

- LOFAR's long wavelength & large bandwidth = **unprecedented precision**
(see Burn 1966, Brentjens & de Bruyn 2005)



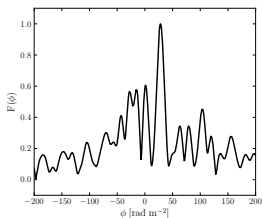
Effelsberg 100-m

$\Delta t = 15$ min

$\nu = 1347$ MHz

$\Delta\nu = 200$ MHz

FWHM = 260 rad m⁻²



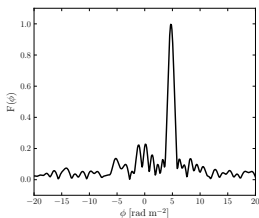
WSRT

$\Delta t = 20$ min

$\nu = 350$ MHz

$\Delta\nu = 80$ MHz

FWHM = 12 rad m⁻²



LOFAR full core HBA

$\Delta t = 10$ min

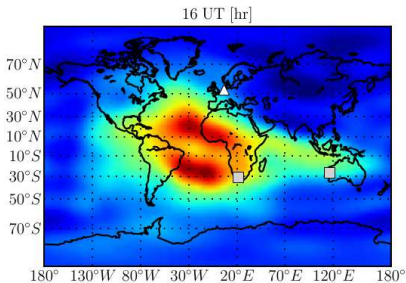
$\nu = 163$ MHz

$\Delta\nu = 68$ MHz

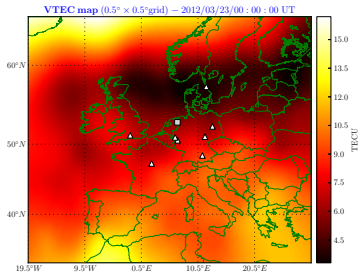
FWHM = 1.2 rad m⁻²

Ionospheric RM

- Ionosphere also magnetised plasma
- $\Delta PA = (RM_{\text{ion}} + RM_{\text{ISM}} + RM_{\text{IGM}} + RM_{\text{int}})\lambda^2$
- ionFR: ionospheric RM toward LOS using TEC maps & IGRF11 (Sotomayor-Beltran, Sobey et al. 2013 A&A)



- CODE; 2 hrs, $5^\circ \times 2.5^\circ$



- ROB; 15 mins, & $0.5^\circ \times 0.5^\circ$

Ionospheric RM variation

- Ionosphere dynamic on minute to yearly time-scales
- Time & position dependent calibration required

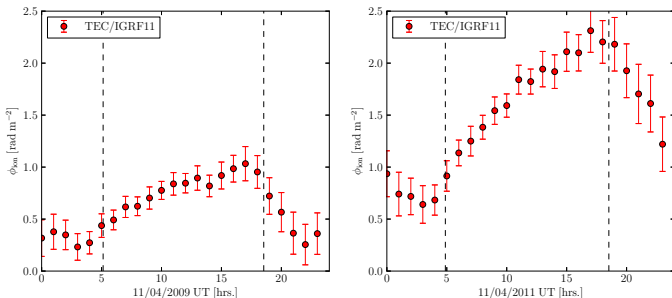


Figure: Daily RM variation as viewed from LOFAR Superterp toward Cassiopeia A. [Sotomayor-Beltran et al. 2013]

Ionospheric RM variation: yearly

- Weekly averages of the maximum (blue) and minimum (red) absolute ionospheric RM
- Correction essential for monitoring RMs
- 280 pulsars 300 pc above/below galactic plane: median RM $\sim 39 \text{ rad m}^{-2}$

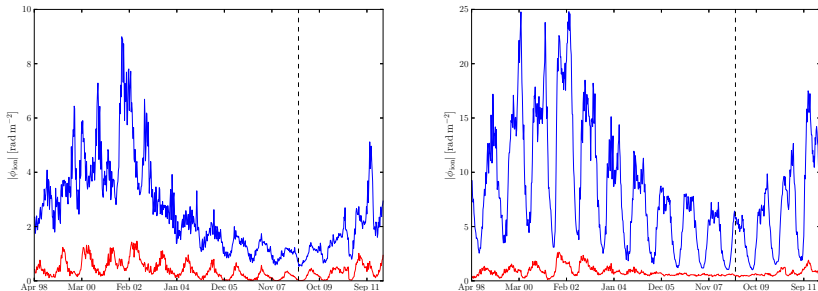


Figure: *left:* towards CasA viewed from LOFAR; *right:* towards Eta Carinae viewed from average of Western Australian and South African SKA core sites. [Sotomayor-Beltran et al. 2013]

LOFAR observations and model comparison I

- Pulsar observed multiple times over several hrs using LOFAR Superterp – RM(time)

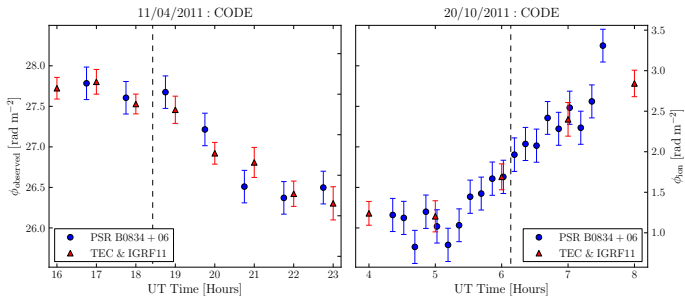


Figure: *left:* B0834+06 observed 7×10 mins every hour on 11th April 2011 over sunset at 120–126 MHz; *right:* B0834+06 observed 20×3 mins every 10 mins on 20th October 2011 over sunrise at 129–140 MHz. [Sotomayor-Beltran et al. 2013]

LOFAR observations and model comparison II

- Three pulsars observed over several hrs quasi-simultaneously using Superterp
- Comparison for 3 LOSs with large angular separation ($>60^\circ$)

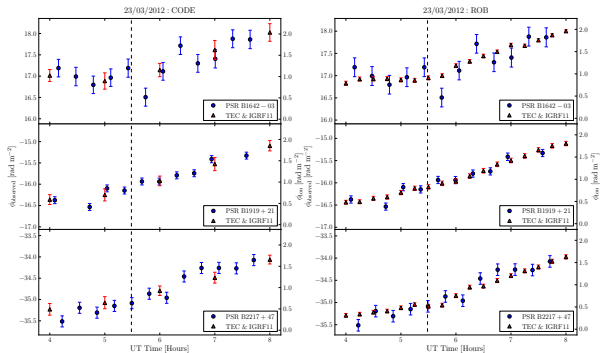


Figure: 12 \times 3 min observations over sunrise; *upper:* PSR B1642–03, 119–125 MHz; *mid:* PSR B1919+21 58–64 MHz; *lower:* PSR B2217+47 119–125 MHz. *left:* CODE data, *right:* ROB data. [Sotomayor-Beltran et al. 2013]

Preliminary ionosphere-calibrated LOFAR RMs

<i>PSR</i>	<i>ObsID</i>	RM_{ISM}^{LOFAR}	σ_{RM}^{LOFAR}	RM_{ISM}^{psrcat}	σ_{RM}^{psrcat}	<i>ref</i>	$\langle B_{\parallel} \rangle_{ne}^{LOFAR}$	$\sigma_{\langle B_{\parallel} \rangle}^{LOFAR}$
		$rad\ m^{-2}$	$rad\ m^{-2}$	$rad\ m^{-2}$	$rad\ m^{-2}$		μG	μG
B0031-07	L77919	+9.85	0.09	+9.8	0.2	hl87	1.07	0.01
B0136+57	L77917	-93.7	0.1	-90	4	hl87	-1.565	0.002
B0809+74	L77929	-13.9	0.1	-11.7	1.3	man72	-2.79	0.02
B0809+74	L78237	-13.9	0.1	-11.7	1.3	man72	-2.79	0.02
B0823+26	L78236	+5.3	0.1	+5.9	0.3	man74	0.338	0.006
B0834+06	L78235	+25.2	0.1	+23.6	0.7	hl87	2.41	0.01
B0950+08	L78234	+1.47	0.09	-0.66	0.04	jhv+05	0.61	0.04
J1012+5307	L78453	+2.9	0.1	*	*	*	0.40	0.01
J1012+5307	L81268	+2.9	0.1	*	*	*	0.40	0.01
J1022+1001	L81050	+1.29	0.08	-0.6	0.5	ymv+11	0.16	0.01
B1133+16	L78233	+3.87	0.09	+1.1	0.2	jhv+05	0.98	0.02
B1237+25	L78449	-0.22	0.09	-0.33	0.06	tml93	-0.03	0.01
B1257+12	L78454	+7.70	0.09	*	*	*	0.93	0.01
B1508+55	L78448	+1.5	0.1	+0.8	0.7	man72	0.092	0.006
B1911-04	L77835	+3.94	0.09	+4.4	0.9	jhv+05	0.0543	0.001
B1919+21	L77912	-16.9	0.1	-16.5	0.5	hl87	-1.68	0.01
B1929+10	L77913	-6.93	0.09	-6.87	0.02	jhv+05	-2.68	0.03
B1953+50	L77897	-23.69	0.09	-22	2	hl87	-0.913	0.003
B1953+50	L77928	-23.7	0.1	-22	2	hl87	-0.916	0.004
B2021+51	L77910	-6.7	0.1	-6.5	0.9	man72	-0.369	0.006
B2111+46	L77909	-221.9	0.1	-224	2	man72	-1.935	0.001
J2145-0750	L78171	-1.9	0.1	-1.3	0.7	ymv+11	-0.27	0.02
B2217+47	L77908	-35.8	0.09	-35.3	1.8	man72	-1.013	0.002
B2224+65	L77907	-22.9	0.1	-21	3	hl87	-0.781	0.003

RMs projected on H-alpha

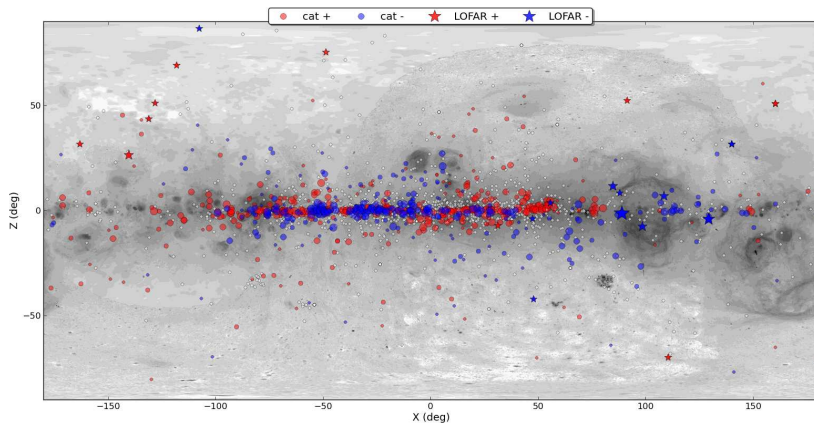


Figure: RMs from psrcat (Manchester et al. 2005) and LOFAR projected on H-alpha map (Finkbeiner et al. 2003 & refs therein)

Ongoing Work

- Ongoing cycle 0 obs $|RM| \leq 10$ – attain more precise data (table)
- Ongoing cycle 0 obs MSPs etc with no known RMs

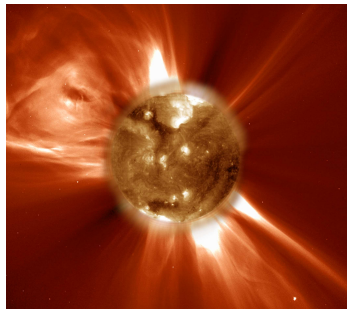
<i>PSR</i>	<i>P</i> <i>s</i>	<i>DM</i> <i>pc cm⁻³</i>	<i>RM</i> _{ISM} ^{psrcat} <i>rad m⁻²</i>	$\sigma_{RM}^{\text{psrcat}}$ <i>rad m⁻²</i>	<i>S</i> ₄₀₀ <i>mJy</i>	<i>dist</i> <i>kpc</i>
B0037+56	1.118225	92.59	9.00	13	7.50	4.48
B0301+19	1.387584	15.74	-8.30	0.3	27.00	0.95
B0402+61	0.594576	65.30	9.00	3	15.00	3.05
B0450+55	0.340729	14.49	10.00	3	59.00	1.18
J0538+2817	0.143158	39.57	-7.00	12	8.20	1.30
B0540+23	0.245975	77.71	8.70	0.7	29.00	3.54
B0751+32	1.442349	39.95	-7.00	5	8.00	3.92
B0823+26	0.530661	19.45	5.90	0.3	73.00	0.32
B0950+08	0.253065	2.96	-0.66	0.04	400.00	0.26
B1112+50	1.656440	9.20	3.20	0.5	12.00	0.54
B1133+16	1.187913	4.86	1.10	0.2	257.00	0.35
B1237+25	1.382449	9.24	-0.33	0.06	110.00	0.84
B1508+55	0.739682	19.61	0.80	0.7	114.00	2.10
B1530+27	1.124836	14.70	1.00	0.3	13.00	0.98
B1839+56	1.652862	26.70	-3.00	3	21.00	1.70
B1905+39	1.235757	30.96	7.00	3	23.00	1.76
B1923+04	1.074078	102.24	0.00	11	22.00	3.95
B1929+10	0.226518	3.18	-6.87	0.02	303.00	0.31
B2021+51	0.529197	22.65	-6.50	0.9	77.00	1.80
B2310+42	0.349434	17.28	7.00	2	89.00	1.06

Future Work

- Continue LOFAR observations of nearby known pulsars
- Follow-up observations of newly discovered pulsars
- Highly complimentary for detecting magnetic fields in, e.g., globular clusters and the heliosphere
- Future polarisation observations to use pulsar RMs for calibration?



Hubble space telescope image of M15 [P. Guhathakurta et al., NASA, ESA]



The Sun and Coronal mass ejection [SOHO Consortium, ESA, NASA]

Aside: element beam

- Pulsar S/N over time – discuss necessary observations during busy days?

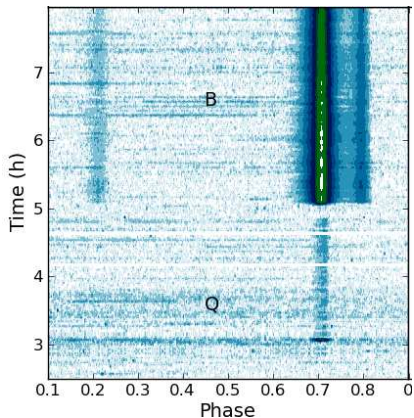


Figure: 8-hr LOFAR HBA observation of B0823+26 (21 core stations, 110–188 MHz)